Bis(monoacylglycero)phosphate accumulation in macrophages induces intracellular cholesterol redistribution, attenuates liver-X receptor/ATP-Binding cassette transporter A1/ATP-binding cassette transporter G1 pathway, and impairs cholesterol efflux.

Céline Luquain-Costaz, Etienne Lefai, Maud Arnal-Levron, Daria Markina, Shota Sakaï, Vanessa Euthine, Asami Makino, Michel Guichardant, Shizuya Yamashita, Toshihide Kobayashi, et al.

Bis(monoacylglycero)phosphate accumulation in macrophages induces intracellular cholesterol redistribution, attenuates LXR/ABCA1/ABCG1 pathway and impairs cholesterol efflux

Céline Luquain-Costaz*, Etienne Lefai*, Maud Arnal-Levron*, Daria Markina*, ShotaSakaï[†], Vanessa Euthine*, Asami Makino[†], Michel Guichardant*, Shizuya Yamashita[‡], Toshihide Kobayashi[†], Michel Lagarde*, Philippe Moulin*and Isabelle Delton-Vandenbroucke*

Université de Lyon, UMR 1060 Inserm (CarMeN), Institut National des Sciences Appliquées (INSA)-Lyon, Villeurbanne, France (*); Lipid Biology Laboratory, RIKEN, Saitama, Japan ([†]); Department of Cardiovascular Medicine, Osaka University Graduate School of Medicine, Osaka, Japan ([‡])

Running Title: BMP and LXRs/ABCs pathway in macrophages

Corresponding author: Isabelle Delton-Vandenbroucke, UMR 1060 Inserm (CarMeN), INSA-Lyon, Pasteur-IMBL Building, 20 Ave A. Einstein, 69621 Villeurbanne, France. Tel.: 33-4-72-43-72-36; Fax:33-4-72-43-85-24. E-mail: isabelle.vandenbroucke@insa-lyon.fr.

Key words: lipoproteins, late endosomes, ABC transporters, atherosclerosis, oxysterols

Abbreviations: ABCA1, ATP-binding cassette A1; ABCG1, ATP-binding cassette G1; BMP, bis (monacylglycero)phosphate; CE, cholesterol ester; ER, endoplasmic reticulum; FC, free cholesterol; HMGCoA, hydroxyl,methyl-glutaryl-coenzyme A reductase; LE, late endosomes; LXR, liver-X receptor; MβCD, methyl βcyclodextrin; PG, phosphatidylglycerol; PM, plasma membrane; SREBP, sterol regulatory element-binding protein.

Word count : 5424
Figures: 7
Tables: 2

Basic science, AL

ABSTRACT

Objective- Endosomal signature phospholipid bis(monoacylglycero)phosphate (BMP) has been involved in the regulation of cellular cholesterol homeostasis. Accumulation of BMP is a hallmark of lipid storage disorders and was recently reported as a noticeable feature of oxidized LDL-laden macrophages. This study was designed to delineate the consequences of macrophage BMP accumulation on intracellular cholesterol distribution, metabolism and efflux and to unravel the underlying molecular mechanisms.

Methods and results- We have developed an experimental design to specifically increase BMP content in RAW macrophages. Following BMP accumulation,cell cholesterol distribution was markedly altered despite no change in LDL uptake and hydrolysis, cholesterol esterification, or total cell cholesterol content. The expression of cholesterol regulated genes SREBP2 and HMGCoAR was decreased by 40%, indicative of an increase of endoplasmic reticulum associated-cholesterol. Cholesterol delivery to plasma membrane was reduced as evidenced by the 20% decrease of efflux by cyclodextrin. Functionally, BMP accumulation reduced cholesterol efflux to both apoA1 and HDL by 40%, correlated with a 40% decrease in mRNA contents of ABCA1 and ABCG1 transporters and LXR α and β. Foam cell formation induced by oxidized LDL exposure was exacerbated in BMP enriched cells.

Conclusion-The present work shows for the first time a strong functional link between BMP and cholesterol regulating genes involved in both intracellular metabolism and efflux. We propose that accumulation of cellular BMP might contribute to the deregulation of cholesterol homeostasis in atheromatous macrophages.

INTRODUCTION

Cholesterol cell homeostasis is regulated by a complex set of mechanisms that include cholesterol synthesis, uptake of low density lipoproteins (LDL), cholesterol esterification and cholesterol efflux [1]. The bulk of cholesterol in macrophages originates from receptor-mediated endocytosis of LDL. Macrophages can export excess cholesterol to high-density lipoproteins (HDL) and apolipoprotein A1 (apoA1) by efflux processes that require the activity of adenosine triphosphate (ATP) binding cassette transporter A1 (ABCA1) and ATP binding cassette transporter G1 (ABCG1). During atherogenesis, macrophages take up modified LDL in an unregulated manner, *via* scavenger receptors, ultimately resulting in the deposition of the large stores of cholesteryl esters and free cholesterol that characterize foam cells phenotypes. The formation of cholesterol-laden macrophages is a prominent feature of atherogenesis.

Late endosomes is an obligatory station for LDL-derived cholesterol that is next transported from this organelle to plasma membrane (PM) and endoplasmic reticulum (ER)[2]. Bis(monoacylglycero)phosphate (BMP), sometimes called lysobisphosphatidic acid (LBPA), is a phospholipid highly abundant in the internal membranes of multivesicular late endosomes, in which it forms specialized lipid domains [3]. Several reports have demonstrated the involvement of BMP in both structure and function of late endosomes/lysosomes (reviewed in [4]). We and others have underlined the role of BMP in cellular cholesterol transport and distribution. It was first reported that treatment of cultured fibroblasts with anti-BMP antibody that accumulates in late endosomes resulted in a massive accumulation of cholesterol in this compartment [3, 5]. The modulation of BMP domains by the glycolipid inhibitor D-threo-1-phenyl-2-decanoylamino-3-morpholino-1-propanol (D-PDMP) altered cellular cholesterol homeostasis in these cells [6]. More recently, it was demonstrated that the cholesterol exit and retention in late endosomes depends on BMP content in this compartment, through a mechanism involving the endosomal protein Alix[7]. Our studies in both murine and human macrophages showed that endosomal accumulation of anti-BMP antibody altered cholesterol distribution in relation with reduced cholesterol efflux to HDL[8].

Most human and animal cells or tissues contain relatively low amounts of BMP, not exceeding 1-2% of total phospholipids. However, the level of BMP was shown to dramatically increase in certain inherited lysosomal storage disorders (LSD), a group of diseases characterized by endolysosomallipidosis such as Niemann-Pick (NP) and Gaucher diseases (reviewed in [4]). Gaucher disease, that displays lipid engorged cells of the monocyte-macrophage lineage, has been associated with low HDL cholesterol concentration evocating a deregulation of cholesterol homeostasis [9]. Furthermore, BMP accumulation has been recently reported as a noticeable feature of oxidized LDL-laden macrophages [10].

To date, literature dealing with the understanding of cholesterol-related functions of BMP is rather scarce. We previously reported that cellular BMP content was significantly increased after incubation of RAW 264.7 macrophages with the precursor dioleoyl-phosphatidylglycerol (18:1/18:1-PG)[11]. This approach was considered as a valuable model of BMP accumulation regarding that BMP produced from exogenous PG by RAW macrophages has been shown to keep the unique sn1:sn1' stereoconfiguration of natural BMP [12]. In addition, we here report that 18:1/18:1-BMP was primarily increased after supplementation with 18:1/18:1-PG, thus mimicking the conditions found in LSD for both cellular and plasma BMP accumulation [13]. Our results show for the first time that endosomal BMP accumulation impacts on cholesterol distribution and efflux in association with changes in cholesterol regulating genes. Molecular mechanisms involving LXR/ABCA1/ABCG1 are proposed to contribute in the effects of BMP on cholesterol homeostasis and especially efflux in macrophages.

MATERIALS AND METHODS

Materials

Tissue culture media were purchased from Eurobio (Les Ulis, France). [1,2,-^{3}H]cholesteryloleate and [1,2,-^{3}H]cholesterol (50 Ci/mmol) were from Perkin Elmer Life Science (Paris, France). Alexa 488 and Alexa 546 were from Molecular Probes (Eugene, OR). Monoclonal antibody against BMP (anti-LBPA antibody, 6C4) was obtained as described [5]. Antibody to the tetraspanin CD63/LAMP3 (clone M13) was from Santa Cruz Biotechnology (CA, USA). 1,2-dioleoyl-*sn*-glycero-3-phospho-*rac*-1-glycerol (18:1/18:1-PG), apoA1, methyl-β-cyclodextrin (MβCD), 3-β-[2-(diethylamino)ethoxy]androst-5-en-17-one(U18666A),stigmasterol and Nile Red , were bought from Sigma (Saint Quentin-Fallavier, France). All solvents were analytical grade from SDS (Peypin, France). Silica gel 60 plates were supplied by Merck (Fontenay Sous Bois, France). Trizol reagent and Superscript II were from Invitrogen (Courtaboeuf, France) and primers from Promega (Charbonnières-les-Bains, France). F1394 was provided by Shizuya Yamashita (Osaka, Japan).

Lipoprotein preparation

Human low-density lipoproteins (LDL) and high-density lipoproteins (HDL) were isolated from plasma by sequential ultracentrifugation. LDL were labeled with [^{3}H]cholesteryloleate or [^{3}H]cholesterol (40 µCi per 1mg LDL protein) as previously described [8].

Cell culture and treatments

Murine macrophage-like RAW 264.7 were obtained from RIKEN Bioresource Center (Tsukuba, Japan). Cells were cultured in MEM supplemented with non essential amino acids, 10% FBS, 2 mM L-glutamine, 100 units/ml penicillin and 100 µg/ml streptomycin and passaged by trypsination. Experiments were started by incubation without (control) or with 30 µM 18:1/18:1-PG liposomes for 24h [11]. Supplementation with 18:1/18:1-PG up to 72h did not affect cell viability (96.2 % ± 3.8 of controls according to colorimetric MTT assay). The incubation with 18:1/18:1-PG was maintained during subsequent incubations with lipoproteins. Incubations with lipoproteins were done in 5% lipoprotein deficient serum (LPDS)-containing medium. Other details of incubation conditions are given below and/or in figure legends.

LDL uptake and LDL-associated CEhydrolysis

Cells were incubated with 50 µg/ml of [^{3}H]cholesteryloleate-LDL. Aliquot of cell lysates (in 0.1% Triton) was counted by liquid scintillation and LDL uptake was calculated as nCi/mg cell protein. Total lipids were extracted from cell lysates by the method of Bligh and Dyer [14]. [^{3}H]FC (free cholesterol) and [^{3}H]CE (cholesterol esters) were separated by TLC (hexane/diethyl ether/acetic acid, 80/20/1, *v/v*) and detected with a radioactivity analyzer (Raytest, France). LDL-associated CE hydrolysis was assayed as the percentage of total radioactivity recovered as [^{3}H]FC.

Cholesterol Esterification

Cells were incubated with 50 µg/ml of [^{3}H]cholesterol-LDL. The distribution of [^{3}H]FC and [^{3}H]CE was analyzed as detailed above. Cholesterol esterification was expressed as the percentage of total radioactivity recovered as [^{3}H]CE. Cholesterol esterification was also evaluated by the conversion of [^{3}H]FC to [^{3}H]CE in cells labeled with [^{3}H]FC (1 µCi/ml).

Free cholesterol (FC) and cholesterol esters (CE) content

Cells were incubated in basal culture conditions or in presence of 100µg/ml LDL (loading conditions) for 12h. Total lipids were extracted from cell lysates, and sterols (FC, CE) were separated by TLC (hexane, diethyl ether, methanol, acetic acid, 50/50/5/1, *v/v*). FC was measured by GC-MS using stigmasterol as an internal standard [15].CE was measured by GC of fatty acid methyl esters using cholesterylheptadecanoate as an internal standard [8].

Cholesterol efflux to HDL, apoA1 and mβCD
Cells were pre-incubated with 50 µg/ml of [^{3}H]cholesteryloleate-LDL or 1 µCi/ml [^{3}H]cholesterol for 12 h. Cholesterol efflux was then stimulated by incubation with 10 mM MβCD, 100 µg/ml HDL or 10 µg/ml apoA1 + 0.5 mM 8 BrcAMP[16] in 5% LPDS-containing medium. The radioactivity in cells and in media was determined by liquid scintillation counting. More than 95% of the radioactivity in media was recovered as FC. Cholesterol efflux was expressed as the percentage of radioactivity released into the medium relative to total radioactivity in cells plus media. The values correspond to the net efflux after subtraction of spontaneous efflux measured in 5% LPDS-medium.

Quantification of BMP and PG species by LC-MS
An Agilent 1100 series LC (Agilent Technologies, Santa Clara, CA) coupled to a 4000 QTRAP hybrid triple quadrupole mass spectrometer (AB SCIEX, Foster City, CA) was used to quantify the individual BMP and PG species. Extracted lipids (2 µl) were injected onto a reversed phase C18 column (CAPCELL PAK C18 MG III, 2.0 × 50 mm, Shiseido CO., LTD., Tokyo, Japan) and were eluted with an isocratic flow (100 µl/min) of methanol : acetonitrile (90:10) containing 5 mmol/L ammonium formate and 0.1% formic acid. MS analysis was run in the positive ion mode Multiple-reaction monitoring (MRM) mode was used to measure the PG and BMP species, containing different acyl chains. BMP and PG contents in cells were calculated by relating the peak areas of each species to the peak area of the corresponding internal standard (C14:0/C14:0-BMP or C14:0/C14:0-PG) and the standard curve of each internal standard (0-20 pmol). Data acquisition and analysis were performed using Analyst Software version 1.4.1 (AB SCIEX).

Foam cell formation assay
Macrophages were plated on coverslips and incubated with 50 µg/mL oxidized LDL (10 µM $CuSO_4$, 37°C, 5h) for 24h, rinsed three times with PBS, and then fixed at room temperature for 20 min with 4% para-formaldehyde. Macrophages were then rinsed twice with PBS and stained 30 min at room temperature with 0.1µg/ml Nile Red. Cells were rinsed twice with PBS, mounted and observed under Olympus IX81 microscope. Fluorescence intensity was determined using cell^Fsoftware (Soft Imaging System).

BMP staining
Cells were fixed and stained with Alexa 488– or Alexa 546-conjugated primary antibodies (anti-BMP (6C4) and anti-CD63 antibodies) as described [8]. The specimens were mounted with Mowiol and examined under Zeiss LSM 510 confocal microscope equipped with the C-Apochromat 63XW Korr (1.2 n.a.) objective.

Quantification of mRNAs by real-time RT-PCR
Cells were incubated in basal culture conditions or in presence of 100µg/ml LDL (loading conditions) for 12h. Total RNA was isolated using the Trizol reagent according to manufacturer's instructions. First-strand cDNAs were synthesized from 500 ng of total RNAs in the presence of 100 U of Superscript II and a mixture of random hexamers and oligo(dT) primers. Real-time PCR assays were performed with Rotor-GeneTM 6000 (Corbett Research, Mortlake, Australia). A list of the primers and real-time PCR assay conditions are available upon request (lefai@univ-lyon1.fr). The results were normalized using HPRT mRNA concentration, measured as a reference gene in each sample.

Statistical analysis
Data are presented as mean values ± SD. All statistical analyses were performed using the JMP 10.0.2 software (SAS Institute, Inc.). Multiple comparisons were performed by one-way ANOVA. Means comparisons of all pairs were performed by the Tukey-Kramer Honestly Significant Difference method based on ANOVA with $\alpha = 0.05$; significantly different pairs are indicated in the figures by different capital letters. Comparisons of experimental means from

two groups were performed by unpaired Student's *t*-test; significant differences at $p \leq 0.05$ and $p \leq 0.001$ are indicated in the figures by * and ***, respectively.

RESULTS

Supplementation with 18:1/18:1-PG induced the specific accumulation of BMP in late endosomes.

We previously reported that supplementation of cultured RAW macrophages with 30 µM of 18:1/18:1-PG liposomes induced cellular accumulation of BMP with no change in other PL, namely phosphatidylcholine and phosphatidylethanolamine[11]. We here further show that PG content did not change in this condition whereas BMP content was increased by 2-fold (Figure 1A). The conversion of PG to BMP in RAW macrophages requires a PG-selective phospholipase A_2 whose activity towards 16:0/16:0-PG is low compared to oleate-containing PG [17]. Consistently, we found that BMP content was unchanged in cells supplemented with 30 µM of 16:0/16:0-PG whereas PG content was significantly increased. Total PG plus BMP reached similar amounts in both 16:0/16:0-PG and 18:1/18:1-PG supplemented cells, about twice that in controls (7333, 7889 and 3799 pmol/mg protein for the two added PG and control samples, respectively) indicating that both PG were taken by the cells at equal rate, with no conversion of 16:0/16:0-PG and total conversion of 18:1/18:1-PG to BMP. As shown in Table 1, 18:1/18:1-BMP was the major BMP molecular species in 18:1/18:1-PG supplemented cells. Overall, molecular species composition of BMP in these cells was similar to control cells. Supplementation with 16:0/16:0-PG resulted in a large increase in 16:0/16:0-PG at the expense of other PG molecular species (Table 2), which confirms previous reports indicating that 16:0/16:0-PG was not metabolized in RAW macrophages.

The intracellular distribution of BMP was visualized with the anti-BMP antibody (6C4) (Figure 1B). The endosomal localization of BMP in control RAW macrophages is supported by the co-localization with the tetrapanin CD63, a late endosome marker. BMP immunofluorescence in 18:1/18:1-PG supplemented cells revealed a punctuated and perinuclear staining similar to control cells and co-localized with CD63, supporting an endosomal location of newly synthesized BMP.

Supplementation with 18:1/18:1-PG liposomes was then used as a model of specific endosomal BMP accumulation, as referred to BMP-enriched cells, in the next experiments.

BMP accumulation does not modify LDL-derived cholesterol delivery to macrophages

Free cholesterol (FC) delivery to macrophages after LDL endocytosis depends on both LDL uptake, hydrolysis of LDL-associated cholesteryl esters (CE) in the late endosomal/lysosomal compartment and cholesterol re-esterification in the endoplasmic reticulum (ER) by ACAT (acetyl-CoA acetyltransferase). No difference in LDL uptake, as assessed using [^{3}H]cholesteryloleate-LDL, was observed between control and BMP-enriched cells (Figure 2A). Hydrolysis of LDL-associated CE was measured in presence of 2 µg/ml ACAT inhibitor F1394 to avoid cholesterol re-esterification. At this concentration, F1394 led to complete inhibition of cholesterol esterification as assayed by [^{3}H]oleate incorporation test (not shown). Figure 2B indicates similar rate of CE hydrolysis in both control and BMP-enriched cells. Cholesterol esterification was measured as the proportion of radioactivity recovered in CE after incubation with [^{3}H]cholesterol-LDL or [^{3}H]cholesterol. In all tested conditions, no difference was observed between control and BMP-enriched cells (Figure 2C). These data suggest no change in the esterification process after BMP accumulation.

Cellular levels of FC and CE were also quantified (Figure 2D). In basal conditions (unloaded), FC content was slightly increased ($\simeq$+10 %, $p \leq 0.05$) in BMP-enriched cells compared to controls. After loading with LDL, FC content was increased by about 40% compared to basal conditions, and no effect of BMP accumulation could be observed. CE contents were similar in control and BMP-enriched cells in basal conditions, and equally increased (about 3-fold) after loading with LDL. These data indicate no or only minor change in cellular FC and CE contents in BMP-enriched cells, at least at the whole cell level.

Altogether, these results indicate that BMP accumulation does not alter LDL internalization

and hydrolysis nor subsequent cholesterol re-esterification.

BMP accumulation is associated with redistribution of LDL-derived cholesterol.

The consequences of BMP accumulation on LDL-derived cholesterol transport to plasma membrane (PM) and ER were examined. We previously showed that cholesterol efflux to methylβcyclodextrin (MβCD) is indicative of the proportion of LDL-derived cholesterol transported to the plasma membrane in RAW macrophages [8]. As shown in Figure 3A, cholesterol efflux to MβCD was significantly reduced in BMP-enriched cells compared to controls for (≃-20 %, $p \leq 0.05$), suggesting a decreased transport of cholesterol to PM.

The content of cholesterol in ER is known to regulate the expression of SREBP2 and SREBP2 target genes like HMGCoAreductase[18]. As expected, cell loading with LDL which is assumed to increase ER cholesterol, significantly decreased SREBP2 mRNA level (≃-40 % *vs*. controls, p=0.0016) (Figure 3B). Treatment with U18666A (1µg/ml) which has been reported to inhibit cholesterol transport to ER in many cells including RAW macrophages [8, 19] consistently reversed LDL-induced suppression of SREBP2 and increased SREBP2 expression above control values (1.4-fold *vs*. controls, p=0.024). Conversely, LDL-induced suppression of SREBP2 was exacerbated in BMP-enriched cells (≃-80 % *vs*. control, $p<0.0001$ and ≃-60 % *vs*. LDL, p=0.0014). Similar variations were observed for HMGCoAreductase mRNA (Figure 3C). These results suggest that BMP accumulation is associated with increase in ER cholesterol.

BMP accumulation decreased HDL- and apoA1-stimulated cholesterol efflux

Macrophages were then challenged for their capacity to release cholesterol in response to HDL and apoA1 after cell loading with LDL. As shown in Figure 4A, both HDL- and apoA1-stimulated efflux were reduced by ≃ 40% in BMP-enriched cells compared to controls ($p<0.0005$ and $p<0.001$, respectively). Significant diminution of HDL-stimulated cholesterol efflux could be observed throughout time-course experiments (Figure 4B). As control for BMP specificity, cholesterol efflux to HDL was measured in PG-enriched cells (supplemented with 16:0/16:0-PG) and no difference was observed with controls (20.7± 2.3 *vs.* 22.3 ± 2.2 %, respectively, mean ± SD of 3 determinations).

Data from mβCD-mediated cholesterol efflux (Figure 3A) suggest that the transport of LDL-derived cholesterol to PM is decreased in BMP-enriched cells, which could explain the lower cholesterol efflux in LDL-loaded cells. In another series of experiments, cells were incubated with free [^{3}H]cholesterol that can exchange with plasma membrane and label cellular pools independent of LDL loading. A decrease of cholesterol efflux to HDL and apoA1 was then observed in BMP-enriched cells compared to controls (HDL: -52%, $p<0.0005$, apoA1: -46%, $p<0.05$) (Figure 4C). Altogether, these results suggest that the decrease in LDL-derived cholesterol efflux in BMP-enriched cells did not result from lower cholesterol availability in PM.

Decreased expression of ABCA1 and ABCG1 transporters and LXR receptors is involved in the decreased cholesterol efflux in BMP-enriched cells

HDL and apoA1-stimulated efflux of cholesterol in macrophages have been shown to essentially depend on the expression/activity of ABC transporters G1 and A1, respectively [20, 21]. As shown in Figure 5 A and 5B, loading with LDL increased ABCA1 and ABCG1 mRNA levels, by 4 and 2-fold, respectively, *vs* controls ($p<0.0001$). These results are *per se* important since previous studies have only reported induced expression of ABCA1 and ABCG1 in murine macrophages upon loading with acetylated/oxidized LDL [22, 23]. Our present data therefore indicate that exposure to native LDL alone is sufficient to increase expression of both ABCA1 and ABCG1, although to a lower extent compared to modified LDL. Noteworthy, ABCA1 expression was significantly reduced in BMP-enriched cells in both basal conditions (18:1/18:1-PG *vs* controls, -70%, p=0.038) and after LDL loading

(LDL+18:1/18:1-PG *vs* LDL, -70%, $p<0.0001$) (Figure 5A). Similar effects were obtained for ABCG1 (18:1/18:1-PG *vs* controls, -47%, p=0.012 and LDL+18:1/18:1-PG *vs* LDL, -49%, $p<0.0001$) (Figure 5B). The decrease in basal expression of these transporters may explain the decrease of cholesterol efflux observed in cells labeled with [^{3}H]FC (Fig 4C). As control for BMP specificity, ABCG1 expression was measured in PG-enriched cells (supplemented with 16:0/16:0-PG) and no significant difference was observed *vs*controls (85.0 ± 17.3 vs 85.8 ± 7.2, relative values, mean ± SD of 3 determinations) which is consistent with unchanged cholesterol efflux to HDL in these cells. Altogether, these data indicate that lowered cholesterol efflux to HDL and apoA1 could result from the decreased expression of ABCA1 and G1 transporters.

Because ABCA1 and ABCG1 are target genes of liver X receptors (LXRs) α and β in RAW macrophages [22, 23], we also studied the putative involvement of LXRs in the decrease of cholesterol efflux in BMP enriched cells. To evaluate the role of LXR activators, cells were treated with the LXR ligand 22(R)hydroxy-cholesterol (22(R)) in association with retinoic acid (RA), resulting in the induction of both ABCA1 and ABCG1 genes (not shown). As illustrated in Figure 5C, LXR activation triggered significant apoA1-mediated cholesterol efflux and enhanced HDL-mediated efflux (50% *vs.* 25% in control non treated cells, *cf*. Figure 4A,). Under these conditions, cholesterol efflux was similar in both control and BMP-enriched cells, indicating that 22(R)/RA was able to reverse the effects of BMP accumulation. The expression of LXRs was also examined (Figure 5D and 5E). As previously reported [22, 23], LXRβ is more highly expressed than LXRα in RAW macrophages. Loading with LDL increased both LXRα (1.3-fold, p=0.0012) and LXRβ (1.4-fold, p=0.016) mRNA levels. LXRα expression was significantly reduced in BMP-enriched cells upon LDL loading (LDL+18:1/18:1-PG *vs* LDL, -50%, $p<0.0001$) and in basal conditions although to a lower extent (18:1/18:1-PG *vs* controls, -22%, p=0.0014) (Figure 5D). Similar effects were obtained for LXRβ (LDL+18:1/18:1-PG *vs* LDL, -65%, $p<0.0001$ and 18:1/18:1-PG *vs* controls, -29%, p=0.045) (Figure 5E). These effects paralleled those observed for ABCA1 and ABCG1, suggesting that a down regulation of LXRs could participate in down-regulating these ABC transporters. Again, no difference was observed in PG-enriched cells (supplemented with 16:0/16:0-PG) *vs* controls (LXRα, 42.2 ± 4.3 vs 40.7 ± 2.2, and LXRβ, 247 ± 39 vs 203 ± 8, relative values, mean ± SD of 3 determinations) which is consistent with unchanged expression of ABCA1 and G1 transporters in these cells.

OxLDL-induced foam cell formation is exaggerated in BMP enriched cells

Another functional consequence of BMP accumulation was evaluated by foam cell formation assay. As expected, Nile red positive cells were significantly increased after exposure to oxidized LDL compared to controls (oxLDL*vs* controls, +30%, $p<0.0001$) (Figure 6A and 6B). Most importantly, Nile red staining was further enhanced in BMP-enriched cells (oxLDL+18:1/18:1-PG *vs* controls, +48%; oxLDL+18:1/18:1-PG *vs*oxLDL, p=0.007), indicating that BMP accumulation contributes to foam cell formation. As control for BMP specificity, Nile red staining was measured in PG-enriched cells (supplemented with 16:0/16:0-PG) and no difference was observed with cells exposed to oxLDL only.

DISCUSSION

Our current study reveals not only the suppressive effects of BMP accumulation on cholesterol efflux in macrophages but also the underlying molecular mechanisms. Indeed, we demonstrated that BMP accumulation reduces the expression of key cholesterol regulatory genes including ABCA1, ABCG1, SREBP2 and SREBP2 dependent genes. We further connect the regulation of ABC transporters to the LXR pathway with the putative involvement of LXR ligand oxysterols. Furthermore, we draw a possible link between BMP accumulation and atherogenesis through the exacerbated foam cell formation in BMP-enriched cells.

Our conclusions are established from studies based on the supplementation with 18:1/18:1-PG to induce BMP accumulation in RAW macrophages. Interesting studies from the Gruenberg's team have been previously done in BHK cells and fibroblasts using exogenous BMP provided by liposomes. By this approach, the authors were able to compare different BMP molecular species and/or BMP with different stereo-configurations and demonstrated that both of these structural characteristics were relevant for BMP functions [7]. In our study, the aim was to evaluate the consequences of increased BMP closest to natural BMP. According to previous data, PG was converted into BMP with the natural sn-1:sn-1' stereo-configuration in RAW macrophages[12] and we here show that molecular species composition of BMP was not significantly changed after supplementation with 18:1/18:1-PG. Furthermore, accumulated BMP was recovered in late endosomes. Importantly, we can reasonably conclude that BMP accumulation is responsible for the reported effects since key effects, like cholesterol efflux and ABCG1 expression, were not reproduced under supplementation with 16:0/16:0-PG that accumulated in cells but was not converted to BMP.

Previous works including from our group have highlighted the involvement of BMP in the regulation of cholesterol transport, especially in respect to exit/retention in the endosome-lysosome compartment [5-8]. Our present study examined the cholesterol distributionin downstream compartments including PM and ER. We thereby showed that BMP accumulation compromised LDL-derived cholesterol transport to PM. Based on the repression of SREBP2 and HMG-CoA reductase in BMP-enriched cells, we also concluded that BMP accumulation is associated with an increase in ER cholesterol content. In apparent contradiction, LDL uptake was not modified in BMP-enriched cells, while the expression of LDL receptor is known to be regulated by the SREBP2 pathway. Recent studies have reported that LDL receptor could be degraded by Idol (inducible degrader of the LDLR, an E3 ubiquitin ligase) whose expression is controlled by LXR [24]. Since LXRs are repressed in BMP-enriched cells, one possible mechanism is a less Idol-dependent degradation of LDL receptor, which could compensate for its putative suppression by the SREBP2 pathway. Also surprising in respect to increased ER cholesterol is the fact that cholesterol esterification was not increased in BMP-enriched cells, suggesting that ER cholesterol accumulation would then specifically impact on SREBP2 and SREBP-dependent genes. It could be that these genes respond to smaller variation of ER cholesterol content as compared to ACAT activity. Alternatively, it has been suggested that specific FC pools in ER could be involved for ACAT activation [25] and this pool may not be modified in BMP-enriched cells.

Mechanisms responsible for altered distribution of cholesterol to ER and PM are quite difficult to investigate since pathways of intracellular cholesterol trafficking at the molecular level are poorly understood [26]. It is however assumed that the Niemann-Pick type C (NPC) proteins NPC1 and NPC2 are involved in the normal egress of cholesterol out of LE [27, 28] and several studies have suggested functional interaction between BMP and NPC proteins [7,27]. While it is generally accepted that ABCA1 functions in cholesterol efflux at the plasma membrane, it has been suggested that localization and trafficking of ABCA1 into intracellular compartments including late endosomes may play an important role in modulating ABCA1 transporter activity [29-31]. The possibility that BMP accumulation in LE affects ABCA1 trafficking through this organelle is thus to investigate. Previously, we reported that anti-BMP antibody altered LDL-derived cholesterol distribution in RAW macrophages [8]. Further experiments have revealed cholesterol redistribution amongst plasma membrane specific cholesterol pools (unpublished observations). Together with our present data, these observations support the hypothesis that endosomal BMP is important for normal targeting of cholesterol to functional pools.

One major functional consequence of BMP accumulation is the suppressive effects on both HDL and apoA1-stimulated cholesterol efflux, which correlated with the repression of ABCG1 and ABCA1 transporters. The contribution of oleoyl moieties in the down-expression of ABC transporters in BMP-enriched cells (i.e. supplemented with 18:1/18:1-PG) should be

considered regarding that unsaturated fatty acids including oleic acid have been shown to repress these transporters [32, 33], or to be inactive [34, 35]. When exerting suppressive effects, oleic acid was supplied as a non-esterified fatty acid at relatively high concentrations (from 0.1 to 1 mM), which is several order of magnitude higher than in our experimental conditions (esterified oleate, 30 µM PG). LXRs data are also informative in this respect as BMP accumulation attenuated the expression of LXRs whereas oleic acid was reported to have no effect [32]. All these observations weaken the possibility that oleic acid alone mediates the effects of 18:1/18:1-PG.
In contrast to BMP accumulation, antibody blocking BMP did not change the expression of cholesterol regulating genes ABCA1, ABCG1, SREBP, and LXRs (*not shown*). Reduced cholesterol efflux by anti-BMP antibody may then rather result, as mentioned above, from cholesterol redistribution amongst plasma membrane specific cholesterol pools not available to HDL.

ABCA1 and ABCG1 transporter genes are well known targets of LXRs, whose regulation depends on several parameters, including protein synthesis and activation by ligands [36]. Very little is known about the regulation of LXRs expression. Our data indicate that both LXRα and LXRβ genes are induced after loading with native LDL. Since LDL-induced LXRs expression was reduced by BMP-enriched cells, we propose that down-regulation of LXRs contributes to the down-regulation of ABCA1 and ABCG1 genes. This hypothesis is supported by the fact that over-expression of LXRα is correlated to increased expression of both ABCA1 and ABCG1 in RAW macrophages [22]. Deactivation of LXRs by a lack of ligand is another possible mechanism since the decreased cholesterol efflux in BMP-enriched cells was reversed in presence of LXR activators. To further investigate LXR activation pathway, we attempted to measure the cellular content of 25-hydroxycholesterol (25-HC) and 27-hydroxycholesterol (27-HC), two potent ligands of LXRs receptors [36]. However, both 25-HC and 27-HC were detected at very low levels in control cells and were not increased upon LDL loading, not supporting their involvement in LXR activation [37]. Another potent LXR activator is 24(S),25-epoxycholesterol, a unique oxysterol in that it is produced through a shunt of the mevalonate pathway for cholesterol. Several studies have shown that inhibition of 24(S),25-epoxycholesterol synthesis is correlated with ABCA1 down-regulation whereas stimulation induced up-regulation [38-40]. Of specific interest, it was proposed that SREBP2 is required for the synthesis of 24(S),25-epoxycholesterol [41]. Since we found that expressions of SREBP2 and HMG-CoA reductase were decreased in BMP-enriched cells, one would expect a decrease in 24(S),25-epoxycholesterol in these cells which could lead to lower LXR activation and ABCA1 and ABCG1 down-regulation. Further research in this area is certainly warranted and should provide better understanding in the role of endogenous oxysterols in the LXR/ABCA1-ABCG1 pathway in macrophages.

In conclusion our findings shed some light on the still enigmatic late endosomal phospholipid BMP. We propose a functional link between endosomal BMP and the LXR/ABCA1/ABCG1 pathway underlying the effects of BMP on the regulation of cholesterol homeostasis in macrophages. (Figure 7). Of pathophysiological relevance, we show that foam cell formation induced by oxLDL was exaggerated in BMP-enriched cells, supporting a role of BMP in atherogenesis.

SOURCES OF FUNDING
This work was supported by grants from INSA-Lyon, Inserm, and RIKEN at Tokyo-Wako.

Acknowledgments
The authors are grateful to Gerard Febvay(UMR 203, BiologieFonctionnelle, Insecteset Interactions (BF2I) INRA, INSA-Lyon) for help and advice in statistical analyses.

DISCLOSURES

none

REFERENCES

1. Maxfield FR, van Meer G. Cholesterol, the central lipid of mammalian cells. *Curr Opin Cell Biol*. 2010;22:422-429
2. Brooks DA. The endosomal network. *Int J Clin Pharmacol Ther*. 2009;47 Suppl 1:S9-17
3. Kobayashi T, Beuchat MH, Lindsay M, Frias S, Palmiter RD, Sakuraba H, Parton RG, Gruenberg J. Late endosomal membranes rich in lysobisphosphatidic acid regulate cholesterol transport. *Nat Cell Biol*. 1999;1:113-118
4. Hullin-Matsuda F, Luquain-Costaz C, Bouvier J, Delton-Vandenbroucke I. Bis(monoacylglycero)phosphate, a peculiar phospholipid to control the fate of cholesterol: Implications in pathology. *Prostaglandins Leukot Essent Fatty Acids*. 2009;81:313-324
5. Kobayashi T, Stang E, Fang KS, de Moerloose P, Parton RG, Gruenberg J. A lipid associated with the antiphospholipid syndrome regulates endosome structure and function. *Nature*. 1998;392:193-197
6. Makino A, Ishii K, Murate M, Hayakawa T, Suzuki Y, Suzuki M, Ito K, Fujisawa T, Matsuo H, Ishitsuka R, Kobayashi T. D-threo-1-phenyl-2-decanoylamino-3-morpholino-1-propanol alters cellular cholesterol homeostasis by modulating the endosome lipid domains. *Biochemistry*. 2006;45:4530-4541
7. Chevallier J, Chamoun Z, Jiang G, Prestwich G, Sakai N, Matile S, Parton RG, Gruenberg J. Lysobisphosphatidic acid controls endosomal cholesterol levels. *J Biol Chem*. 2008;283:27871-27880
8. Delton-Vandenbroucke I, Bouvier J, Makino A, Besson N, Pageaux JF, Lagarde M, Kobayashi T. Anti-bis(monoacylglycero)phosphate antibody accumulates acetylated ldl-derived cholesterol in cultured macrophages. *J Lipid Res*. 2007;48:543-552
9. de Fost M, Langeveld M, Franssen R, Hutten BA, Groener JE, de Groot E, Mannens MM, Bikker H, Aerts JM, Kastelein JJ, Hollak CE. Low hdl cholesterol levels in type i gaucher disease do not lead to an increased risk of cardiovascular disease. *Atherosclerosis*. 2009;204:267-272
10. Orso E, Grandl M, Schmitz G. Oxidized ldl-induced endolysosomal phospholipidosis and enzymatically modified ldl-induced foam cell formation determine specific lipid species modulation in human macrophages. *Chem Phys Lipids*. 2011;164:479-487
11. Bouvier J, Zemski Berry KA, Hullin-Matsuda F, Makino A, Michaud S, Geloen A, Murphy RC, Kobayashi T, Lagarde M, Delton-Vandenbroucke I. Selective decrease of bis(monoacylglycero)phosphate content in macrophages by high supplementation with docosahexaenoic acid. *J Lipid Res*. 2009;50:243-255
12. Thornburg T, Miller C, Thuren T, King L, Waite M. Glycerol reorientation during the conversion of phosphatidylglycerol to bis(monoacylglycerol)phosphate in macrophage-like raw 264.7 cells. *J Biol Chem*. 1991;266:6834-6840
13. Meikle PJ, Duplock S, Blacklock D, Whitfield PD, Macintosh G, Hopwood JJ, Fuller M. Effect of lysosomal storage on bis(monoacylglycero)phosphate. *Biochem J*. 2008;411:71-78
14. Bligh EG, Dyer WJ. A rapid method of total lipid extraction and purification. *Can J Biochem Physiol*. 1959;37:911-917
15. Benoit B, Fauquant C, Daira P, Peretti N, Guichardant M, Michalski MC. Phospholipid species and minor sterols in french human milks. *Food Chemistry*. 2010;120:684-691
16. Smith JD, Miyata M, Ginsberg M, Grigaux C, Shmookler E, Plump AS. Cyclic amp induces apolipoprotein e binding activity and promotes cholesterol efflux from a macrophage cell line to apolipoprotein acceptors. *J Biol Chem*. 1996;271:30647-30655
17. Shinozaki K, Waite M. A novel phosphatidylglycerol-selective phospholipase a2 from macrophages. *Biochemistry*. 1999;38:1669-1675
18. Bengoechea-Alonso MT, Ericsson J. Srebp in signal transduction: Cholesterol metabolism and beyond. *Curr Opin Cell Biol*. 2007;19:215-222
19. Liscum L, Faust JR. The intracellular transport of low density lipoprotein-derived cholesterol is inhibited in chinese hamster ovary cells cultured with 3-beta-[2-(diethylamino)ethoxy]androst-5-en-17-one. *J Biol Chem*. 1989;264:11796-11806
20. Yvan-Charvet L, Wang N, Tall AR. Role of hdl, abca1, and abcg1 transporters in cholesterol efflux and immune responses. *Arterioscler Thromb Vasc Biol*. 2009;30:139-143
21. Tarling EJ, Edwards PA. Dancing with the sterols: Critical roles for abcg1, abca1, mirnas, and nuclear and cell surface receptors in controlling cellular sterol homeostasis. *Biochim*

Biophys Acta. 2011
22. Venkateswaran A, Laffitte BA, Joseph SB, Mak PA, Wilpitz DC, Edwards PA, Tontonoz P. Control of cellular cholesterol efflux by the nuclear oxysterol receptor lxr alpha. *Proc Natl Acad Sci U S A*. 2000;97:12097-12102
23. Venkateswaran A, Repa JJ, Lobaccaro JM, Bronson A, Mangelsdorf DJ, Edwards PA. Human white/murine abc8 mrna levels are highly induced in lipid-loaded macrophages. A transcriptional role for specific oxysterols. *J Biol Chem*. 2000;275:14700-14707
24. Zelcer N, Hong C, Boyadjian R, Tontonoz P. Lxr regulates cholesterol uptake through idol-dependent ubiquitination of the ldl receptor. *Science*. 2009;325:100-104
25. Sakashita N, Chang CC, Lei X, Fujiwara Y, Takeya M, Chang TY. Cholesterol loading in macrophages stimulates formation of er-derived vesicles with elevated acat1 activity. *J Lipid Res*. 2010;51:1263-1272
26. Mesmin B, Maxfield FR. Intracellular sterol dynamics. *Biochim Biophys Acta*. 2009;1791:636-645
27. Storch J, Xu Z. Niemann-pick c2 (npc2) and intracellular cholesterol trafficking. *Biochim Biophys Acta*. 2009;1791:671-678
28. Peake KB, Vance JE. Defective cholesterol trafficking in niemann-pick c-deficient cells. *FEBS Lett*. 2010;584:2731-2739
29. Neufeld EB, Remaley AT, Demosky SJ, Stonik JA, Cooney AM, Comly M, Dwyer NK, Zhang M, Blanchette-Mackie J, Santamarina-Fojo S, Brewer HB, Jr. Cellular localization and trafficking of the human abca1 transporter. *J Biol Chem*. 2001;276:27584-27590
30. Neufeld EB, Stonik JA, Demosky SJ, Jr., Knapper CL, Combs CA, Cooney A, Comly M, Dwyer N, Blanchette-Mackie J, Remaley AT, Santamarina-Fojo S, Brewer HB, Jr. The abca1 transporter modulates late endocytic trafficking: Insights from the correction of the genetic defect in tangier disease. *J Biol Chem*. 2004;279:15571-15578
31. Kang MH, Singaraja R, Hayden MR. Adenosine-triphosphate-binding cassette transporter-1 trafficking and function. *Trends Cardiovasc Med*. 2010;20:41-49
32. Uehara Y, Engel T, Li Z, Goepfert C, Rust S, Zhou X, Langer C, Schachtrup C, Wiekowski J, Lorkowski S, Assmann G, von Eckardstein A. Polyunsaturated fatty acids and acetoacetate downregulate the expression of the atp-binding cassette transporter a1. *Diabetes*. 2002;51:2922-2928
33. Murthy S, Born E, Mathur SN, Field FJ. Liver-x-receptor-mediated increase in atp-binding cassette transporter a1 expression is attenuated by fatty acids in caco-2 cells: Effect on cholesterol efflux to high-density lipoprotein. *Biochem J*. 2004;377:545-552
34. Wang Y, Oram JF. Unsaturated fatty acids inhibit cholesterol efflux from macrophages by increasing degradation of atp-binding cassette transporter a1. *J Biol Chem*. 2002;277:5692-5697
35. Alvaro A, Rosales R, Masana L, Vallve JC. Polyunsaturated fatty acids down-regulate in vitro expression of the key intestinal cholesterol absorption protein npc1l1: No effect of monounsaturated nor saturated fatty acids. *J Nutr Biochem*. 2010;21:518-525
36. Torocsik D, Szanto A, Nagy L. Oxysterol signaling links cholesterol metabolism and inflammation via the liver x receptor in macrophages. *Mol Aspects Med*. 2009;30:134-152
37. Arnal-Levron M, Chen Y, Delton-Vandenbroucke I, Luquain-Costaz C. Bis(monoacylglycero)phosphate reduces oxysterol formation and apoptosis in macrophages exposed to oxidized ldl. *Biochem Pharmacol*. 2013
38. Wong J, Quinn CM, Brown AJ. Statins inhibit synthesis of an oxysterol ligand for the liver x receptor in human macrophages with consequences for cholesterol flux. *Arterioscler Thromb Vasc Biol*. 2004;24:2365-2371
39. Brown AJ. 24(s),25-epoxycholesterol: A messenger for cholesterol homeostasis. *Int J Biochem Cell Biol*. 2009;41:744-747
40. Beyea MM, Heslop CL, Sawyez CG, Edwards JY, Markle JG, Hegele RA, Huff MW. Selective up-regulation of lxr-regulated genes abca1, abcg1, and apoe in macrophages through increased endogenous synthesis of 24(s),25-epoxycholesterol. *J Biol Chem*. 2007;282:5207-5216
41. Wong J, Quinn CM, Brown AJ. Srebp-2 positively regulates transcription of the cholesterol efflux gene, abca1, by generating oxysterol ligands for lxr. *Biochem J*. 2006;400:485-491

FIGURE LEGENDS

Figure 1. Quantification of BMP and cellular localization. (A) BMP and PG from control cells, 18:1/18:1-PG and 16:0/16:0-PG supplemented cells were quantified by LC-MS as described in Materials and Methods. Data are the mean ± SD of 3 independent determinations. (B) Control and BMP-enriched cells were fixed and stained with Alexa 546-conjugated anti-BMP antibody (6C4) and with Alexa 488-conjugated anti-CD63 antibody .Bar, 10 µm.

Figure 2. Intact cholesterol delivery from internalized LDL in BMP-enriched cells. Control and BMP-enriched cells were incubated with 50 µg/ml [^{3}H]cholesteryloleate-LDL. (A) LDL uptake is expressed as nCi/mg cell protein. (B) CE hydrolysis is expressed as the percentage of [^{3}H]cholesteryloleate converted to [^{3}H]cholesterol in presence of the ACAT inhibitor F1394. (C) Control and BMP-enriched cells were incubated with [^{3}H]cholesterol-LDL or [^{3}H]cholesterol in absence or presence of 100 µg/ml LDL for 12h. Cholesterol esterification was measured as the proportion of radioactivity recovered in CE. (D) Control and BMP-enriched cells were incubated in absence (unloaded) or presence (loaded) of 100 µg/ml LDL for 12h. Sterol contents are expressed as nmol/mg cell protein. Data are the mean ± SD of 4 wells and representative of two independent experiments.

Figure 3. LDL-derived cholesterol redistribution in BMP-enriched cells. (A) Control and BMP-enriched cells were incubated with 50µg/ml of [^{3}H]cholesteryloleate-LDL for 12h. Cholesterol efflux was then stimulated by incubation with 10 mM MβCD for indicated times. (B,C) Control, BMP-enriched cells or U18666A-treated cells were incubated in absence or presence of 100µg/ml LDL for 12h. Cells were analyzed for SREBP2 (B) and HMG-CoA reductase (C) mRNA content as described in Materials and Methods. Data are the mean ± SD of 4-6 wells and representative of three independent experiments.
A, B, C, D, E, significantly different groups (multiple means comparisons by ANOVA and Tukey-Kramer method with α= 0.05).*$p<0.05$ compared to control by t-test.

Figure 4. Decreased cholesterol efflux to HDL and apoA1 in BMP-enriched cells. Control and BMP-enriched cells were incubated with (A,B) 50µg/ml [^{3}H]cholesteryloleate-LDL or (C) 1µCi/ml [^{3}H]cholesterol for 12h. Cholesterol efflux was then stimulated by incubation with (A,C) 100µg/ml HDL for 8h or 10µg/ml apoA1/0.5mM 8brcAMP for 24h; (B) 100µg/ml HDL for the indicated times. Data are the means ± SD of 4 wells and representative of three independent experiments. *$p<0.05$, *** $p<0.001$ compared to control by t-test.

Figure 5. Down-regulation of ABCs and LXRs in BMP-enriched cells. Control and BMP-enriched cells were incubated in absence or presence of 100µg/ml LDL for 12h. Cells were analyzed for ABCA1 (A), ABCG1 (B), LXRα (D) and LXRβ (E) mRNA content. Data are the means ± SD of 4 wells and representative of three independent experiments. *a*, $p\leq0.05$ compared to control, *b*, $p\leq0.05$ compared to LDL. (C) Control and BMP-enriched cells were incubated with 100µg/ml HDL for 8h or 10µg/ml apoA1 for 24h in presence of 2.5µg/ml 22(R)hydroxy-cholesterol/10 µM retinoic acid. Data are the means ± SD of 4-6 wells and representative of three independent experiments.
A, B, C, significantly different groups (multiple means comparisons by ANOVA and Tukey-Kramer method with α= 0.05).

Figure 6. BMP accumulation enhances foam cell formation. Control, BMP and PG-enriched cells were incubated in basal conditions (unloaded) or exposed to 50 µg/mL oxidized LDL for 24h to induce foam cell formation. Cells were fixed and stained with Nile Red. (A) Stained cells were observed through fluorescent microscope and images show representative Nile Red-stained cells. Bar, 25 µm. (B) Quantification of fluorescence was determined using cell^Fsoftware and values represent the means ± SD of four fields. A, B, C, significantly different groups (multiple means comparisons by ANOVA and Tukey-Kramer method with α=

0.05).

Figure 7. Recapitulating scheme of the alterations induced by endosomal BMP accumulation and putative connecting mechanisms.
LDL particles carrying CE are internalized through LDL receptor and reached late endosomes. In this compartment, CE hydrolase (CEH) produces FC that can be transported to other intracellular membranes, such as PM or ER. Incubation of cells with 18:1/18:1-PG liposomes induces an accumulation of 18:1/18:1-BMP into LE, due to the conversion of newly endocytosed-PG (1). BMP accumulation is correlated with FC redistribution: diminution of FC incorporation into PM (2), and increase of FC content in ER (3). ER-FC accumulation induces a suppression of SREBP2 and HMG-CoA reductase expression (4) which could in turn reduce the formation of LXR activator 24(S),25-epoxycholesterol, and thus ABCA1/ABCG1 expression (5), leading to a decrease of FC efflux to HDL and ApoA1 (6). LXR down-regulation may be an additional mechanism to decrease ABCA1/ABCG1 expression (7).

Figure 1

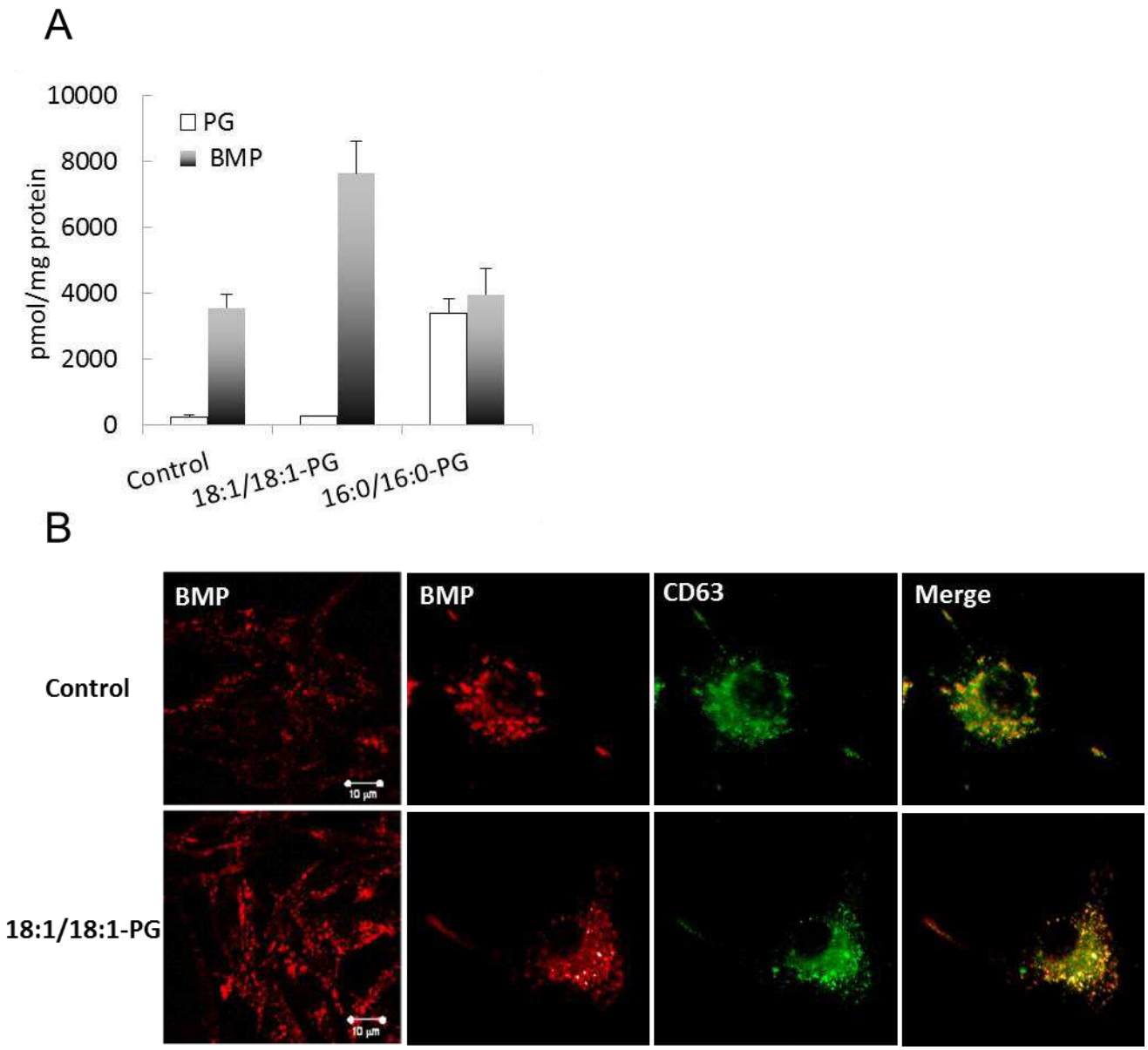
A
10000
8000
6000
4000
2000
0
pmol/mg protein
PG
BMP
Control
18:1/18:1-PG
16:0/16:0-PG
B
Control
18:1/18:1-PG
BMP
BMP
CD63
Merge
10 μm
10 μm

Figure 2

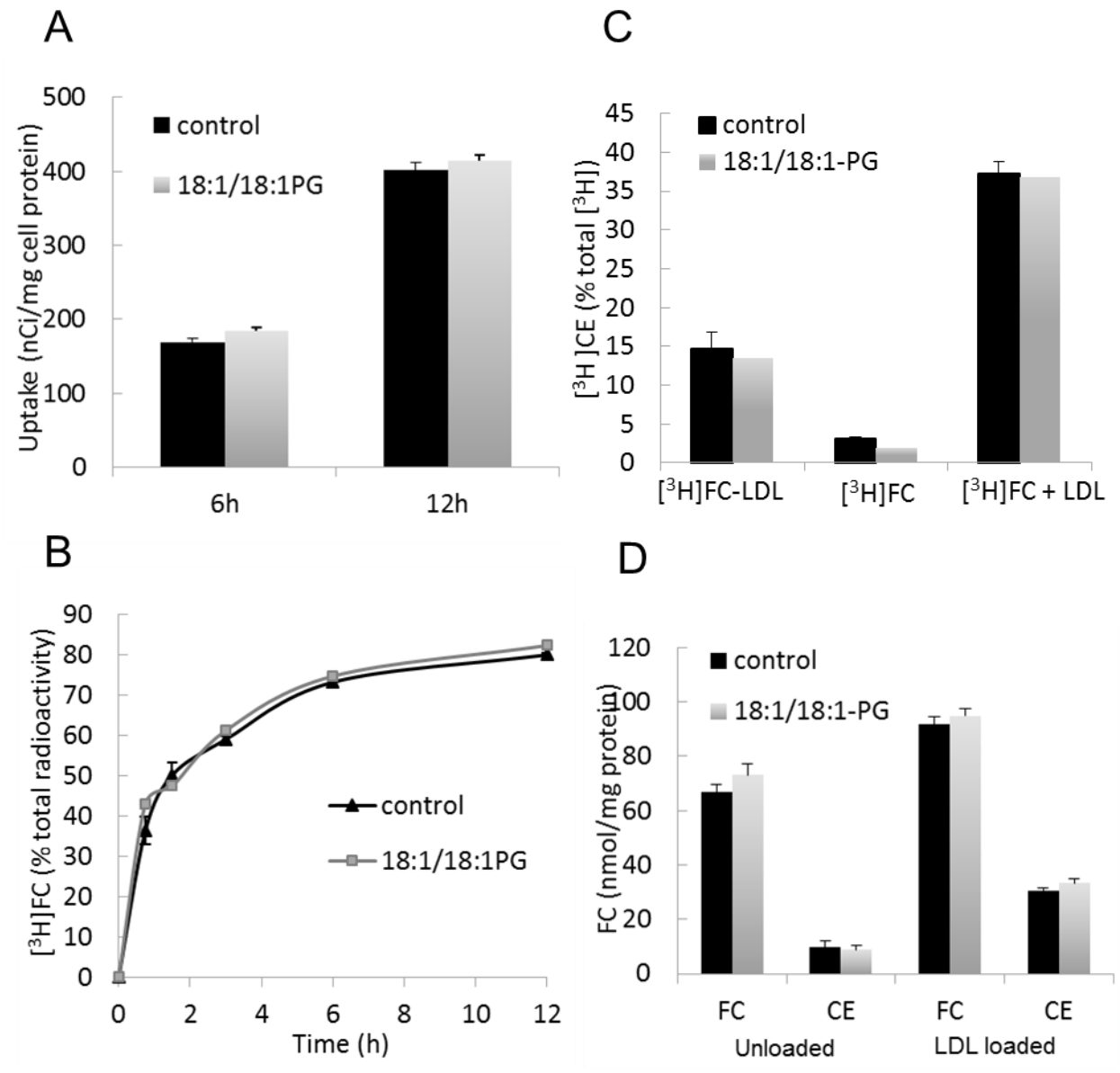
A
Uptake (nCi/mg cell protein)
500
400
300
200
100
0
control
18:1/18:1PG
6h
12h
C
[3H]CE (% total [3H])
45
40
35
30
25
20
15
10
5
0
control
18:1/18:1-PG
[3H]FC-LDL
[3H]FC
[3H]FC + LDL
B
[3H]FC (% total radioactivity)
90
80
70
60
50
40
30
20
10
0
control
18:1/18:1PG
0
2
4
6
8
10
12
Time (h)
D
FC (nmol/mg protein)
120
100
80
60
40
20
0
control
18:1/18:1-PG
FC
CE
FC
CE
Unloaded
LDL loaded

Figure 3

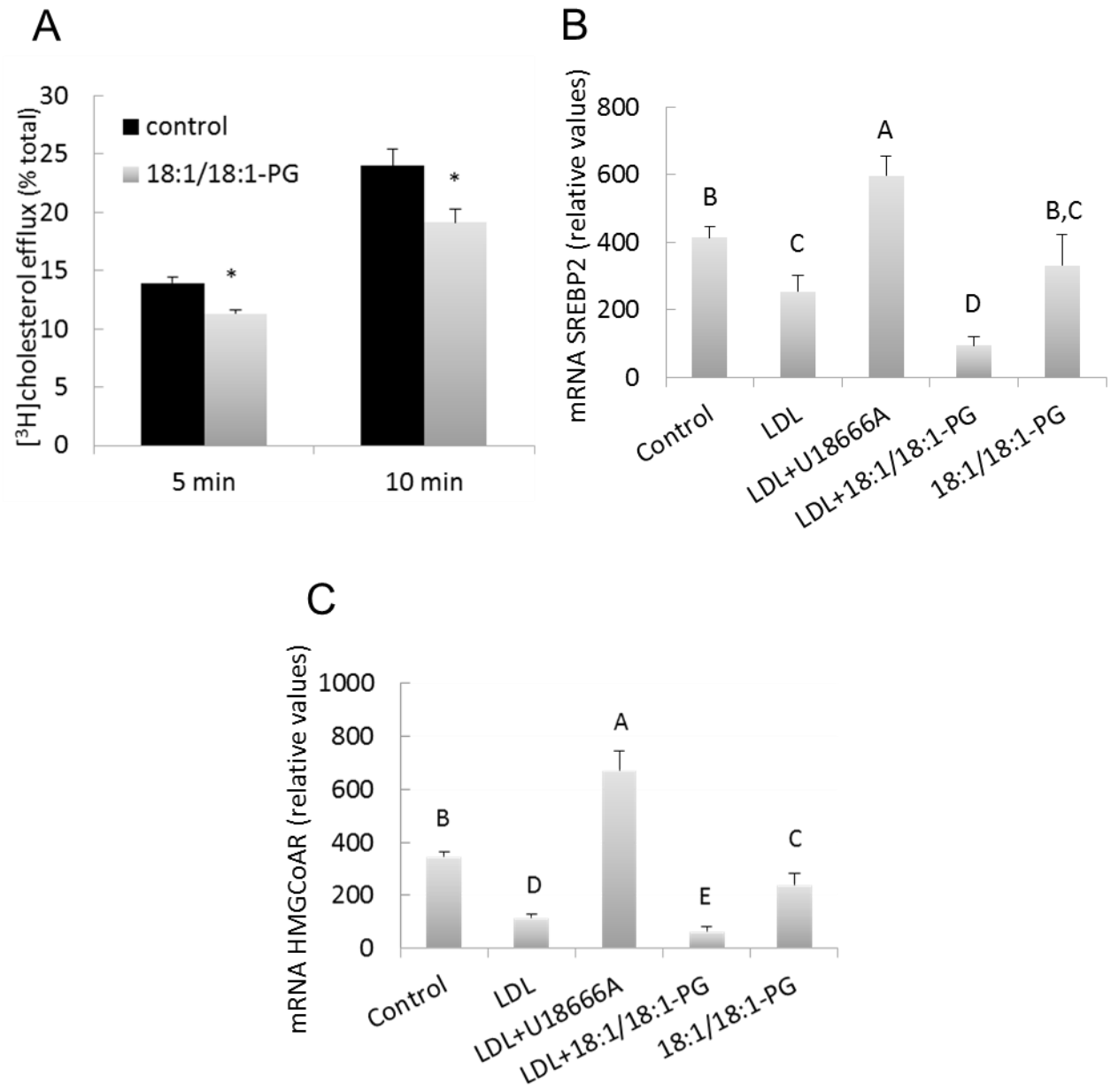
A
[3H]cholesterol efflux (% total)
30
25
20
15
10
5
0
control
18:1/18:1-PG
*
*
5 min
10 min
B
mRNA SREBP2 (relative values)
800
600
400
200
0
B
C
A
D
B,C
Control
LDL
LDL+U18666A
LDL+18:1/18:1-PG
18:1/18:1-PG
C
mRNA HMGCoAR (relative values)
1000
800
600
400
200
0
B
D
A
E
C
Control
LDL
LDL+U18666A
LDL+18:1/18:1-PG
18:1/18:1-PG

Figure 4

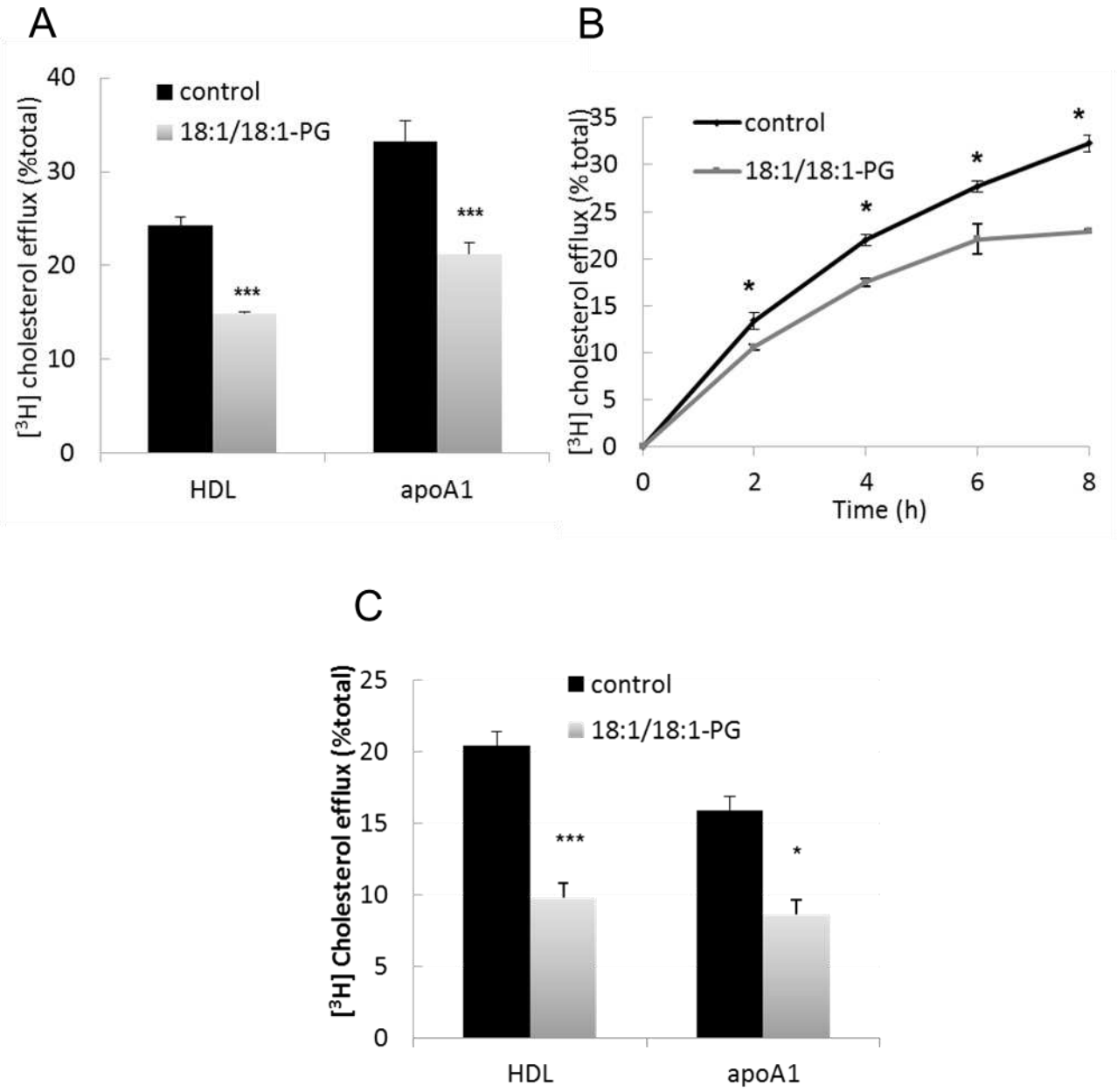
A
40
30
20
10
0
[3H] cholesterol efflux (%total)
control
18:1/18:1-PG
***
***
HDL
apoA1
B
35
30
25
20
15
10
5
0
[3H] cholesterol efflux (% total)
control
18:1/18:1-PG
*
*
*
*
0
2
4
6
8
Time (h)
C
25
20
15
10
5
0
[3H] Cholesterol efflux (%total)
control
18:1/18:1-PG
***
*
HDL
apoA1

Figure 5

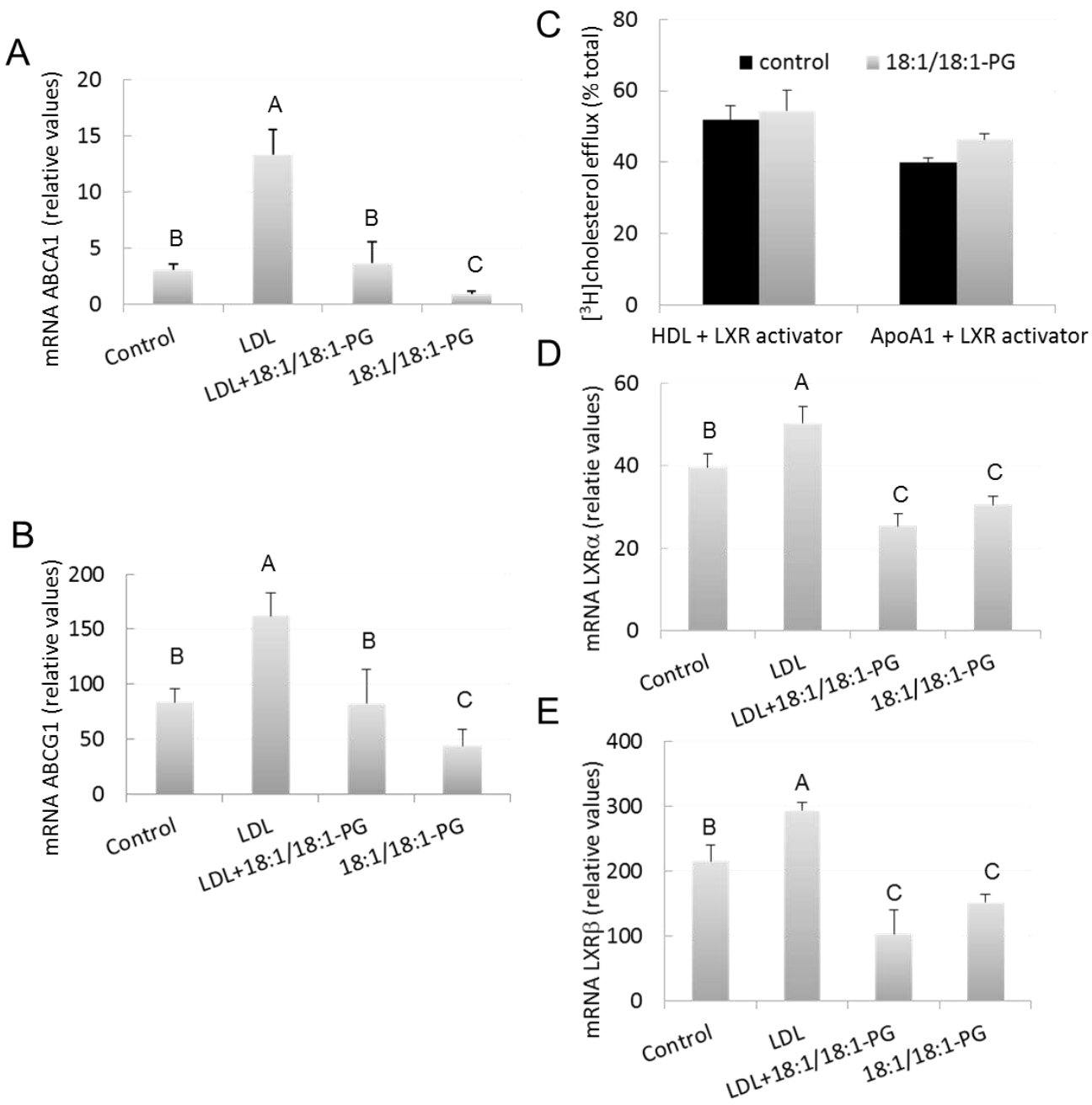
A
mRNA ABCA1 (relative values)
20
15
10
5
0
A
B
B
C
Control
LDL
LDL+18:1/18:1-PG
18:1/18:1-PG
B
mRNA ABCG1 (relative values)
200
150
100
50
0
A
B
B
C
Control
LDL
LDL+18:1/18:1-PG
18:1/18:1-PG
C
[3H]cholesterol efflux (% total)
80
60
40
20
0
control
18:1/18:1-PG
HDL + LXR activator
ApoA1 + LXR activator
D
mRNA LXRα (relatie values)
60
40
20
0
A
B
C
C
Control
LDL
LDL+18:1/18:1-PG
18:1/18:1-PG
E
mRNA LXRβ (relative values)
400
300
200
100
0
A
B
C
C
Control
LDL
LDL+18:1/18:1-PG
18:1/18:1-PG

Figure 6

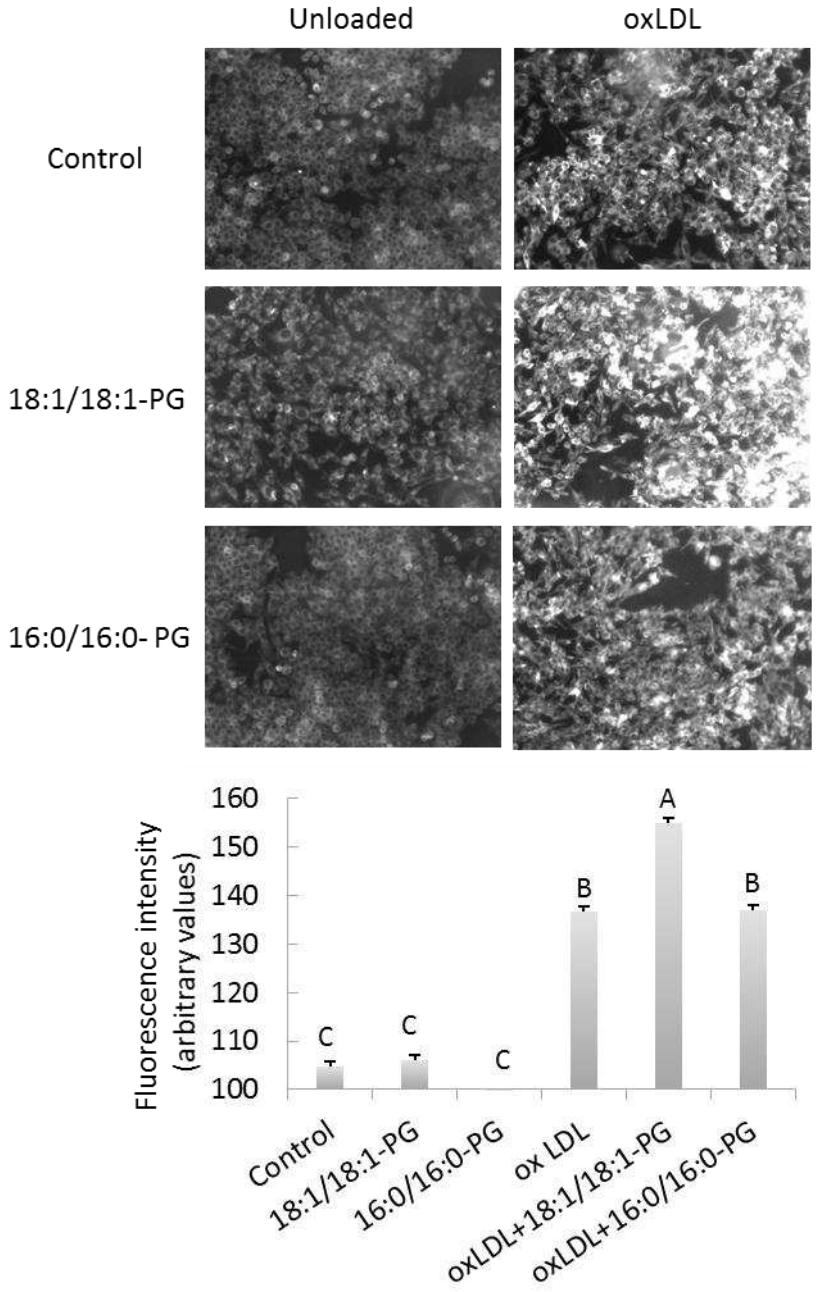
Unloaded
oxLDL
Control
18:1/18:1-PG
16:0/16:0- PG
Fluorescence intensity (arbitrary values)
160
150
140
130
120
110
100
C
C
C
B
A
B
Control
18:1/18:1-PG
16:0/16:0-PG
ox LDL
oxLDL+18:1/18:1-PG
oxLDL+16:0/16:0-PG

Figure 7

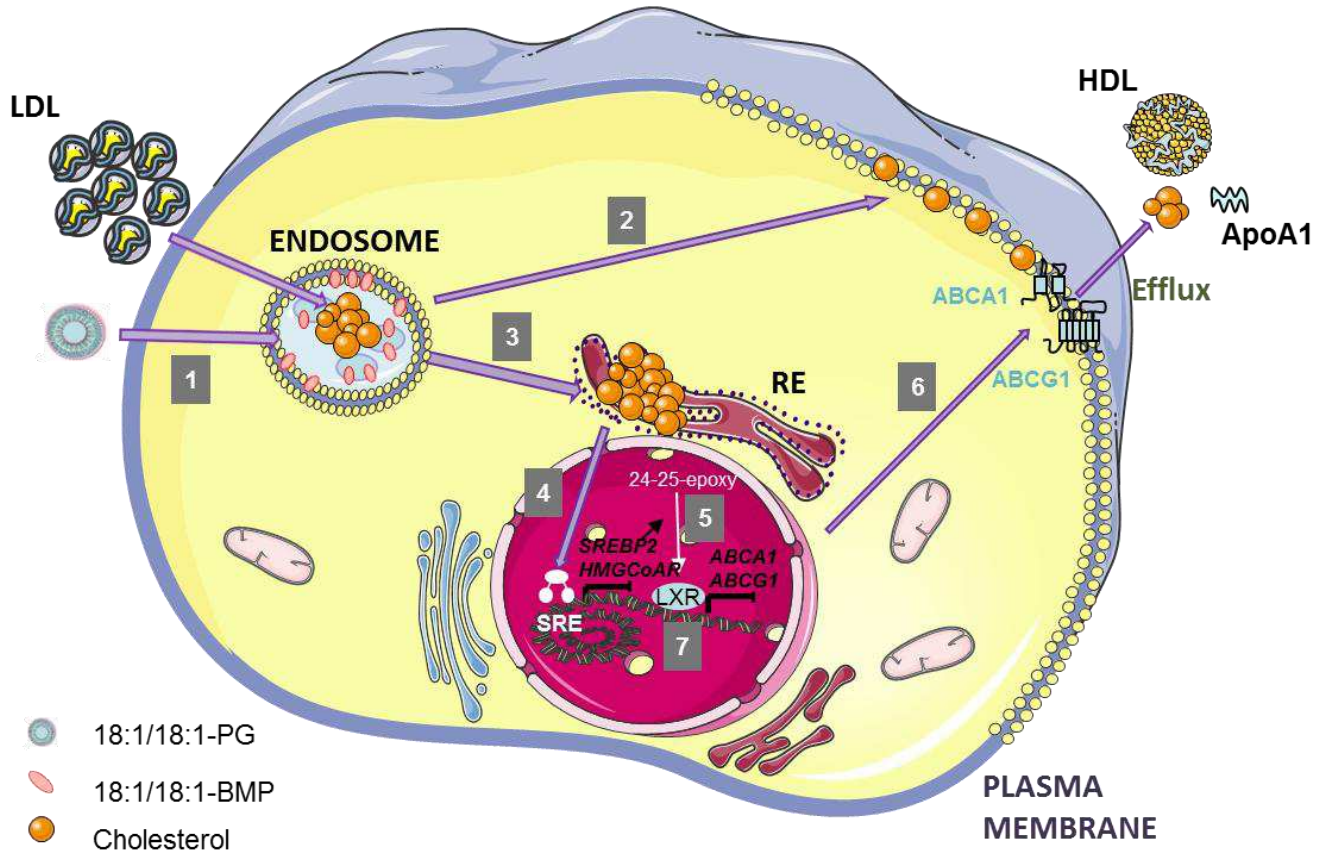
LDL
HDL
ApoA1
ENDOSOME
1
2
3
4
5
6
7
ABCA1
Efflux
ABCG1
RE
24-25-epoxy
SREBP2
HMGCoAR
ABCA1
ABCG1
LXR
SRE
18:1/18:1-PG
18:1/18:1-BMP
Cholesterol
PLASMA
MEMBRANE